



Facile production of CsPbBr₃ perovskite single-crystals in a hydrobromic solution

Murat Özen^{*1}, Cansu Akyel¹, Songül Akbulut Özen²

¹Bursa Technical University, Department of Chemistry, Türkiye

²Bursa Technical University, Department of Physics, Türkiye

Keywords

CsPbBr₃
Perovskite
Single-Crystal
Wet Chemical Synthesis

Research Article

DOI: 10.31127/tuje.1018137

Received: 03.11.2021

Accepted: 31.03.2022

Published: 26.04.2022

Abstract

In this study, synthesis of CsPbBr₃ perovskite single-crystals in a hydrobromic solution was investigated. Single-crystal growth experiments were conducted at the solution-nucleation border at a constant temperature or controlled cooling conditions. Working at the solution-nucleation border poses some practical difficulties such as fast precipitation. Often researchers opt to oversaturate the solution and use the supernatant after filtration. However, for conditions where the A to B ratio in the precursor solution for the formation of ABX₃ is not 1, oversaturation is a waste of resources. In this work, precursor solutions were prepared for a particular working temperature and either held at a constant temperature or were gradually cooled to a predetermined temperature. The constant temperature method resulted in large and clear crystals as it reached saturation more slowly. Crystals prepared at high temperatures appeared to be more transparent with clear facets. Crystals prepared at low temperatures appeared to be opaque with multiple nuclei growth on a single-crystal. Seeding of the saturated solution resulted in larger single-crystals. The procedure adapted in this work made possible the production of clear CsPbBr₃ perovskite single-crystals in a hydrobromic acid solution with sizes of up to 5 mm in only 10 days.

1. Introduction

The need for room temperature operated X - and gamma-ray radiation detectors is becoming more and more important every day, not only for scientific purposes but also for our society. For example, radiation detectors may be used in nuclear (medicine) imaging, radioactivity monitoring, security etc. and are hence crucial for the welfare of modern society [1].

Present commercial semiconductor photodetectors, such as CdTe and CdZnTe, are designed from single-crystal ingots formed as a result of high heat treatments. Superior photodetector properties have been reported for perovskite materials with relatively high absorption, high resistivity, and high charge carrier-charge-life [1].

One of the most prominent perovskite materials that has been investigated for its optoelectronic effects are the hybrid organic perovskites. Although hybrid perovskites possess superior properties - such as large absorption coefficient, high charge carrier mobility, long

electron hole diffusion and tunable band gap - hybrid perovskites are known to be unstable at high temperatures due to the volatile nature of organic cations [2].

Inorganic perovskite materials such as metal lead halides (MPbX₃; M = Cs⁺, X = Cl⁻, Br⁻, I⁻) can be preferred for X-ray and gamma detectors due to their wide band gap (>2.0 eV) and large crystal production. Inorganic metal halide perovskites are emerging as an alternative to hybrid perovskites due to their chemical stability, wide energy range in the spectrum and tunable band gap [2].

Perovskite devices based on polycrystalline materials have low performances due to the existence of many voids, grains boundaries, and surface defect states inside the active perovskites layer. Single-crystal perovskites have been developed largely because of their low trap density and the absence of grain boundaries in them [3]. The need for large, high-quality single-crystalline

* Corresponding Author

^{*}(murat.ozen@btu.edu.tr) ORCID ID 0000-0002-3589-2059
(cansu.akyel@btu.edu.tr) ORCID ID 0000-0003-3509-998X
(songul.akbulut@btu.edu.tr) ORCID ID 0000-0001-8025-2141

Cite this article

Özen, M., Akyel, C., & Özen, S. A. (2023). Facile production of CsPbBr₃ perovskite single-crystals in a hydrobromic solution. Turkish Journal of Engineering, 7(2), 92-98

perovskites is essential to enable research into their practical applications.

Classical solid-state methods such as the Czochralski and Bridgman [4-6] are known to produce large crystals, but these techniques pose limitations such as phase-purity due to temperature dependent crystalline phase transformations. Another limitation of the solid-state methods is its relatively high processing temperature. In this regard, wet chemical methods may offer facile production of photodetector materials due to their low-temperature and ambient pressure conditions.

Centimeter-sized CsPbBr_3 single-crystal synthesis is possible at relatively low temperatures. The inverse temperature crystallization and antisolvent vapor crystallization methods are the most important of the solution-based methods. Dirin et al. [7] have developed several solution-based approaches for the growth of centimeter-scale perovskite single-crystals. Dirin et al. [7] reported the synthesis of CsPbBr_3 single-crystal with low-cost precursors under ambient atmosphere using the inverse temperature crystallization method. Dirin et al. [7] obtained orange, transparent perovskite single-crystals with a radius of 8 mm when the solution was heated to 90-100°C using different solvents such as acetonitrile and methanol in combination with dimethylsulfoxide. Rakita et al. [8] have reported procedures for growing pure CsPbBr_3 crystals of several millimeters in size from a precursor solution. Centimeter-sized single-crystals of CsPbBr_3 were synthesized by solvent-based methods, but it has significant structural defects that greatly reduce its electrical properties.

Hydrohalic solutions can provide easy production of high-quality single-crystal perovskites. Su et al. [9] obtained orange $\text{CH}_3\text{NH}_3\text{PbBr}_3$ single-crystals with sizes of roughly 5 mm produced over a period of 10 days by lowering the solution temperature from 70°C to 50°C. Dang et al. [10] successfully grew a 10 x 10 x 8 mm black and shiny crystal of $\text{CH}_3\text{NH}_3\text{PbI}_3$ at the bottom of the flask after a few days by lowering the solution temperature from 65°C to 40°C. Lian et al. [11] obtained small angular crystals of 3 mm in size by lowering the solution temperature from 100°C to 57°C. They fixed a single-crystal to a platinum wire end, placing it at the bottom of the precursor solution and grew a rhombic dodecahedral MAPbI_3 single-crystal with a size of 12 mm x 12 mm x 7 mm [11].

Hybrid perovskites have been successfully obtained from hydrohalic solutions. However, studies on CsPbBr_3 single-crystals grown in hydrohalic solutions are limited. Dirin et al. obtained CsPbBr_3 single-crystals with dodecahedral shape using Cs:Pb ratio of 1.45 in HBr solution [7]. Peng et al. [12] used an initial Cs:Pb precursor ratio of 1 in order to obtain CsPbBr_3 single-crystals in HBr. To the authors' knowledge, a detailed parametric study of CsPbBr_3 perovskite single-crystals in hydrohalic solutions is lacking in literature. In this study, the synthesis of CsPbBr_3 single-crystals in a hydrobromic solution was investigated. The cooling rate, the synthesis temperature, and the effect of seeded-growth were tested.

2. Method

2.1. Material

Precursor solutions were prepared by dissolving CsBr (99%, Alfa Aesar) and PbBr_2 (98+%, Alfa Aesar) in hydrobromic acid (HBr, aq. 48%, Carlo Erba). All experiments were carried out in an oil bath with precise temperature control on a magnetic hot plate stirrer with the help of thermocouples (See Fig. 1).

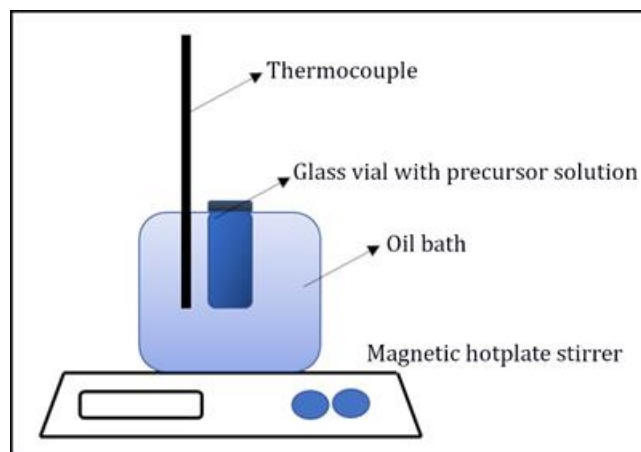


Figure 1. The precursor solution was prepared in an oil bath on a heated magnetic stirrer.

The phase diagram of PbBr_2 :CsBr compositions supports the formation of CsPb_2Br_5 , CsPbBr_3 , Cs_4PbBr_6 [8]. The stoichiometry must be precisely designed to ensure the specific formation of CsPbBr_3 and suppress all other phases. The chemistry behind the Cs to Pb ratio lies in the solubility of the respective ion or ion complexes. In order to reach the desired compositional phase, i.e., CsPbBr_3 , the molar amount of Cs ions – which has a relatively higher solubility in aqueous conditions – needs to be higher than the relatively less soluble Pb ions in aqueous conditions [7]. The Cs:Pb ratio was determined as 1.45 so that the resulting product could only be CsPbBr_3 . Thus, CsBr-rich or PbBr_2 -rich cesium lead bromide phases were avoided.

The synthesis process was finalized by washing the single-crystals with HBr (aq. 48%, Carlo Erba). Afterwards the products were dried and preserved in a desiccator.

2.2. Solubility Test

In order to work at the solution-nucleation border, solubility experiments of CsPbBr_3 were performed in hydrobromic acid by dissolving pre-prepared CsPbBr_3 single-crystals (1 mm and below) at varying temperatures between 30°C and 90°C. Experiments were conducted in glass vials. HBr solutions were heated by means of an oil bath. CsPbBr_3 single-crystals were added to HBr in steps of 0.02 g. The solution was assumed to reach saturation if the last added CsPbBr_3 crystal did not dissolve for 1 hour. The saturation limit was taken as the average weight of crystals added in the last two steps. The appropriate amount of precursor needed at a certain working temperature was determined using the solubility curve in Fig. 2.

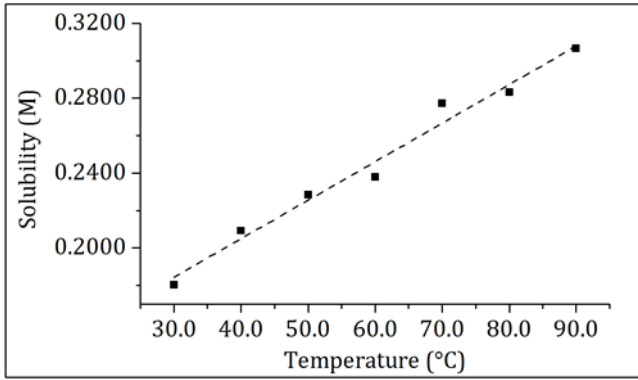


Figure 2. Solubility curve of CsPbBr₃ in HBr (aq. 48%)

2.3. Controlled Temperature Lowering Method

In the controlled temperature lowering method, the temperature of the precursor solution was lowered to the desired final temperature. The glass vial was sealed with a silicone stopper and heated in an oil bath above the saturation temperature. After the precursor was completely dissolved, the solution was cooled to the saturation temperature with a cooling rate of 0.05°C min⁻¹. Once the saturation was reached, the temperature was lowered at a rate of 0.005°C min⁻¹ to avoid multinucleation. The obtained single-crystals were washed with HBr (aq. 48%, Carlo Erba) and dried in a desiccator.

Controlled temperature lowering experiments were carried out at different starting temperatures.

2.4. Constant Temperature Method

In the constant temperature method, the precursor solution was kept at a constant temperature between 30°C and 90°C for a number of days.

2.5. Seeded Growth

In order to grow larger single-crystals, it is crucial to minimize the number of nuclei and use a seed crystal. Hence, a single-crystal of about 1 mm in size was added to a precursor solution and placed at the bottom of the glass vial. Seeded experiments were conducted for both the controlled temperature lowering and constant temperature methods.

2.6. Instrumental

X-ray diffractograms (XRD) were collected with a Bruker AXS/Discovery D8 diffractometer using a Ni-monochromator and Cu-K α radiation ($\lambda=0.1540598$ nm). The tube voltage and the tube current were set at 40 kV and 40 mA, respectively. The scan step size was 0.02 2 θ with 0.5 s per step.

Differential Scanning Calorimetry (DSC) thermograms were recorded under N₂ atmosphere from -75°C to 300°C with a rate of 10°C min⁻¹ using a TA/DSC25 instrument.

The Cs, Pb and Br contents in the prepared single-crystals were analyzed by a Rigaku supermini200X-ray Fluorescence (XRF) Spectrometer and a BrukerTM XFlash 61100 energy dispersive X-ray spectrometer (EDS) instrument.

The obtained CsPbBr₃ single-crystals were visually examined with a Leica M125 light microscope.

UV-VIS-NIR diffuse reflectance measurements of CsPbBr₃ single-crystals were measured in the 200-800 nm range using a SHIMADZU/UV3800 UV-VIS-NIR spectrophotometer. The sample was diluted (5 wt%) in barium sulfate and placed in the sample cup after obtaining a homogeneous mixture. The obtained reflection spectrum was calculated with the Kubelka-Munk equation (Eq.1). Diffuse reflection values were then plotted against the irradiated photon energy $h\nu$ (eV) values by Eq.2. The case where γ is 2 represents the allowed direct electron transfer. The electronic band gap E_g was calculated from the intersection of the linear part with the x-axis in the $(F(R_\infty)h\nu)^2$ versus $h\nu$ graph.

$$F(R) = \frac{(1 - R)^2}{2R} = \frac{K}{S} \quad (1)$$

$$(F(R_\infty)h\nu)^\gamma = A(h\nu - E_g) \quad \text{with } \gamma = 2 \quad (2)$$

3. Results and Discussion

Thermodynamically speaking, single-crystal formation and growth are promoted in a narrow solute concentration area at a specific temperature. By determining the required amount of precursor at a specific temperature, the formation of a single-crystal was aimed without the precipitation of multiple nuclei or polycrystals. For this reason, solubility plots were created for CsPbBr₃ crystals in HBr. The solubility graph that was obtained showed a linear relationship between CsPbBr₃ concentration with increasing temperature (Fig. 2).

Working at the solution-nucleation border does poses some practical difficulties such as fast precipitation. High solute concentrations favor the formation of CsPbBr₃ nuclei, though kinetically speaking dissolution-precipitation mechanisms should also be considered here. Often researchers opt to oversaturate the solution and use the supernatant after filtration. However, for conditions where the A (Cs⁺) to B (Pb²⁺) ratio in the precursor solution is not 1, oversaturation is a waste of resources. In this work, precursor solutions were prepared for a particular working temperature.

Single-crystal growth experiments were conducted at the solution-nucleation border at constant temperature or controlled temperature lowering conditions. The most important aspect of crystallization is undoubtedly temperature and the uniformity thereof. A slight deviation from the predetermined working temperature resulted in multiple nuclei formation. Single-crystal experiments are summarized in Table 1 and Table 2. All single-crystals that were obtained in this work were highly faceted with hexagonal morphologies.

One of the factors that determines the size of single-crystals is the solution's cooling rate. Nucleation is kinetically slowed down at slow heating rates, while high cooling rates trigger rapid nucleation [3]. In this study, multiple small nuclei were formed at relatively high cooling rates. Microscope pictures of CsPbBr₃ single-

crystals are shown in Table 1. At a rate of $0.005^{\circ}\text{C min}^{-1}$ multiple nucleation formation was inhibited and far less nuclei were formed.

Single-crystals that were obtained for experiments conducted from 80°C and 60°C to 40°C resulted in similar average sizes of about 3 mm. Crystal morphologies were hexagonal-shaped. The hexagonal facets were clearly formed for the crystal obtained by cooling from 80°C to 40°C . This was presumed to be due to the longer time spent in the solution. The number of nuclei formed at high starting temperatures were larger. An average of 5 nuclei were formed for the solution prepared by cooling from 60°C to 40°C , while this number was three times higher for the solution cooled from 80°C to 40°C . In both cases clear single-crystals were obtained, though defect formations were also observed. These defect formations are clearly visible in microscope images lit from below the crystal and were thought to be due to the solution's turbidity (see Fig. 3).

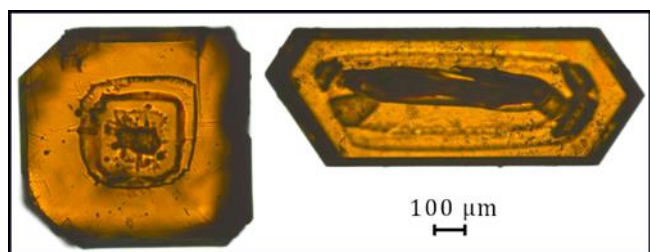


Figure 3. Light microscope images of selected few CsPbBr_3 single-crystals lit from below. Defect formations due to the solution's turbidity are clearly visible inside the single-crystals.

In the constant temperature method, the solution temperature was kept constant for 10 days at 80°C , 60°C and 40°C . Microscope pictures are shown in Table 2. Single-crystals of fairly similar size were obtained (3 mm) irrespective of the temperature. At relatively high temperatures (60°C and 80°C), single-crystal defects became visually apparent due to higher diffusion rates of the ions. Due to the relatively lower thermal energy at 40°C , the resulting single-crystal were clear with far less defects.

In the controlled temperature lowering method, even at extremely low cooling rate of $0.005^{\circ}\text{C min}^{-1}$ equilibrium was continuously disturbed with the potential of multiple nuclei formation.

Larger crystals can be grown by using seed crystals. Seed crystals must have similar crystalline composition as the desired material, i.e., CsPbBr_3 . CsPbBr_3 has the orthorhombic crystalline structure at the synthesis conditions. Large deviations from orthorhombic CsPbBr_3 will cause defects in the final single-crystal.

As previously mentioned, even at low cooling rates equilibrium was continuously disturbed and nucleation was triggered with the formation of multiple small single-crystals. However, less nuclei were observed for seeded experiments. The added seed inhibited the formation of additional nuclei. Furthermore, the final single-crystals were relatively larger compared to those in the unseeded experiments. Single-crystal sizes of up to 5 mm in average were observed for seeded experiments. At conditions where the solution temperature was

lowered from 80°C to 40°C , crystal defect structures were much more pronounced compared to experiments where the solution temperature was lowered from 60°C to 40°C . These differences were attributed to the higher thermal energies of ions in solutions at higher starting temperatures, resulting in more pronounced crystal habit planes.

In contrast, no foreign nuclei were formed for solutions seeded at constant temperature. The grown single-crystal was observed to have a similar morphology to the added seed material. Hence, a good crystalline conformity was obtained between the seed and the final product.

Comparing both the controlled temperature lowering and constant temperature methods, nucleation was observed to be more controllable for constant temperature conditions with regard to the number of nuclei formed during the synthesis. Far less CsPbBr_3 nuclei (about 4 to 5) were formed at constant temperature conditions.

Seeded experiments resulted in the growth of the added seed. A seed crystal with a size of $2\text{ mm} \times 1\text{ mm} \times 1\text{ mm}$ reached a size of $3\text{ mm} \times 3\text{ mm} \times 1\text{ mm}$ when kept at 60°C for 10 days. When cooled from 60°C to 40°C (at $0.005^{\circ}\text{C min}^{-1}$) a seed crystal with a size of $2\text{ mm} \times 2\text{ mm} \times 1\text{ mm}$ grew to a size of $3\text{ mm} \times 2\text{ mm} \times 1\text{ mm}$ in 3 days, which amounted to an average growth of $0.7\text{ mm}^3\text{ day}^{-1}$. At higher temperatures, a seed crystal with a size of $1\text{ mm} \times 1\text{ mm} \times 1\text{ mm}$ reached to a size of $3\text{ mm} \times 2\text{ mm} \times 2\text{ mm}$ when kept at 80°C for 10 days. When cooled from 80°C to 40°C ($0.005^{\circ}\text{C min}^{-1}$), a seed crystal with a size of $2\text{ mm} \times 2\text{ mm} \times 1\text{ mm}$ grew to a size of $5\text{ mm} \times 5\text{ mm} \times 2\text{ mm}$ in only 5 days. This corresponded to a growth rate increase from $1.2\text{ mm}^3\text{ day}^{-1}$ to $9.2\text{ mm}^3\text{ day}^{-1}$. The seed growth rate proved to be faster in the temperature lowering method, especially at higher starting temperatures.

DSC measurement of a well-formed clear CsPbBr_3 single-crystal is shown in Fig. 4. Measurements were taken from -80°C to 300°C at a rate of $10^{\circ}\text{C min}^{-1}$. The first heating cycle (blue) was carried out to remove any possible residues on the sample. The second cooling cycle (red) clearly shows a distinctive peak concurrent with cubic to tetragonal crystal phase transformation (129.8°C) followed by an additional smaller peak, concurrent with the tetragonal to orthorhombic phase transformation at 85.8°C . The third and final heating cycle (green) confirms the crystal phase transformations observed in the second cycle, i.e., orthorhombic to tetragonal crystal phase transformation at 88.7°C and tetragonal to cubic phase transformation at 131.3°C [13]. The DSC graph confirms the phase-pure nature of the obtained CsPbBr_3 single-crystal. DSC measurements of the other CsPbBr_3 samples showed very similar results with clear phase transitions at about 130°C and 85°C .

CsPbBr_3 suffers greatly from phase transitions that occur from cubic to tetragonal at around 130°C and from tetragonal to orthorhombic phase at about 88°C , which can cause mechanical deformations [14]. This is especially true for solid-state procedures that are executed at relatively high temperatures. However, wet-chemical procedures with relatively low synthesis temperatures ($< 80^{\circ}\text{C}$) avoid these issues entirely.

Table 1. CsPbBr₃ single-crystals obtained by the controlled temperature lowering method with a rate of 0.005°C min⁻¹ and a Cs:Pb ratio of 1.45

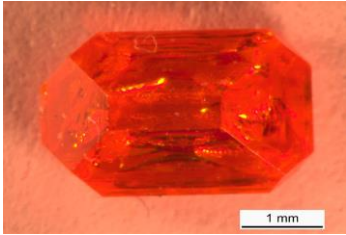
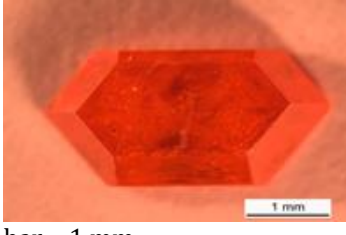
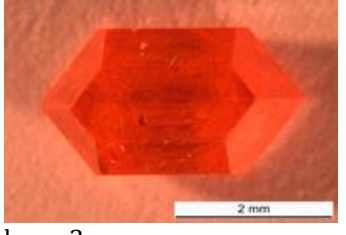
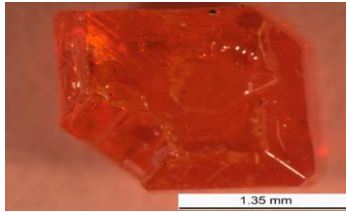
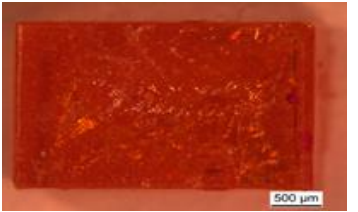
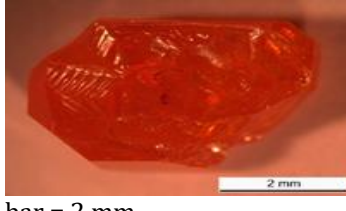
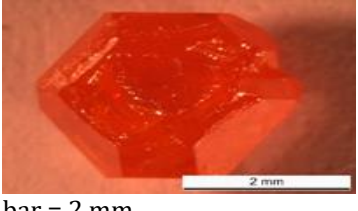
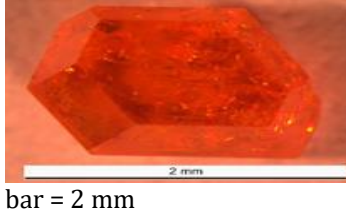
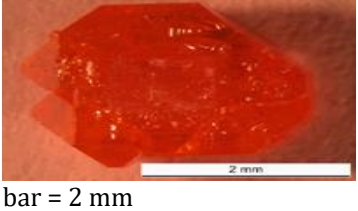
TEMPERATURE	TIME	[Cs] + [Pb]	SEEDLESS	SEEDED
80°C→ 40°C	5 Days	0.283 M	 bar = 1 mm	 bar = 1 mm
60°C→ 40°C	3 Days	0.235 M	 bar = 1 mm	 bar = 2 mm

Table 2. CsPbBr₃ single-crystals obtained by the constant temperature method with a Cs:Pb ratio of 1.4

TEMPERATURE	TIME	[Cs] + [Pb]	SEEDLESS	SEEDED
80°C	10 Days	0.283 M	 bar = 2 mm	 bar = 500 µm
60°C	10 Days	0.235 M	 bar = 2 mm	 bar = 2 mm
40°C	10 Day	0.2092 M	 bar = 2 mm	 bar = 2 mm

The XRD diffractogram of a CsPbBr₃ single-crystal is shown in Fig. 5. The XRD pattern was matched with QualX software [15] to orthorhombic CsPbBr₃ (COD database with ID 00-451-0745) [16]. XRF and EDS elemental analysis results for a CsPbBr₃ single-crystal did show the presence of a slight Cs-excess (Table 3) that, if not originating from the initial CsBr precursor (which is presumed to be washed away with HBr), might point to possible Cs-rich cesium lead bromide phases in the

final product. Furthermore, secondary cesium lead bromide phases were not detected in XRD (Fig. 5), but it should not be forgotten that the instrument's detection limit is about 5%. Any residual secondary phases such as Cs₄PbBr₆ that might have formed during the low temperature syntheses conditions were presumed to be washed away with HBr. XRD diffractograms of all samples matched with orthorhombic CsPbBr₃.

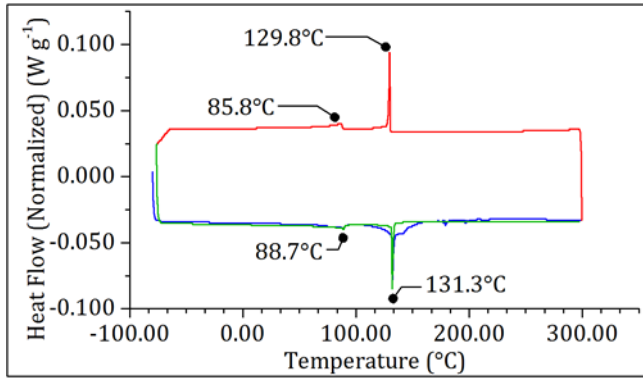


Figure 4. DSC plot of the sample prepared by cooling from 80°C to 40°C (seedless) (Blue plot: -80°C to 300°C, red plot: 300°C to -80°C, green plot: -80°C to 300°C. Measurements were taken at a rate of 10°C min⁻¹).

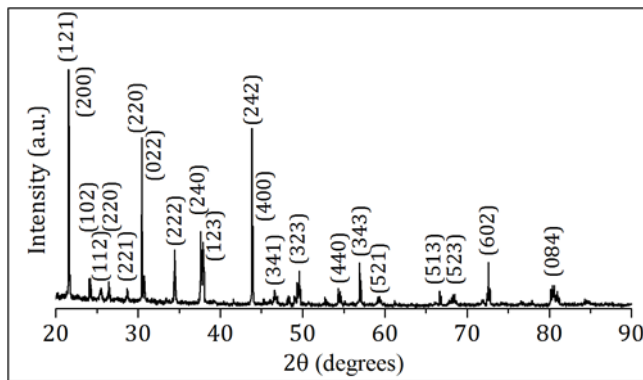


Figure 5. XRD diffractogram of the sample prepared by cooling from 80°C to 40°C (seedless). The pattern was matched with orthorhombic CsPbBr₃ (COD database with ID 00-451-0745) [16]

Table 3. XRF and EDS analysis results of obtained CsPbBr₃ single-crystal

Element	% Mole	
	XRF	EDS
Cs	13.4	17.62
Pb	11.8	16.47
Br	58.1	62.59

Although the XRF values were slightly lower than EDS, both techniques showed that Cs to Pb ratio was close to unity. Excess Cs found with both techniques could be due to the high Cs to Pb ratio (1.45) applied in the initial precursor solution. However, since the solutions were washed with HBr, excess CsBr or even PbBr₂ are unlikely to remain on the single-crystal.

UV-VIS-NIR diffuse reflectance spectroscopy result for a CsPbBr₃ single-crystal is given in Fig. 6. The band gap was calculated using the linear part of the Kubelka-Munk plot. The $F(R)hv^2$ plot has the typical S-like curve and is concurrent with allowed direct band gap semiconductor materials. The Kubelka-Munk plot intersects the x-axis at 2.26 eV, which is concurrent with literature values [17]. All other samples showed similar UV-Vis-NIR diffuse reflectance plots with band gap energies in the 2.2 ± 0.1 eV range. The Kubelka-Munk plot in Fig. 6 shows that CsPbBr₃ is suitable for absorption in the visible spectrum range and high energy photons.

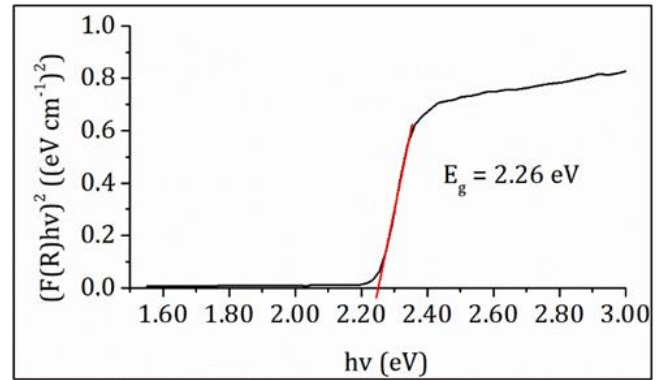


Figure 6. UV-Vis-NIR diffuse reflectance spectrometry measurement of the sample prepared by cooling from 80°C to 40°C (seedless). The linear part of the Kubelka-Munk graph intersects the x-axis at 2.26 eV.

4. Conclusion

To the best of the authors' knowledge, a parametric study on the growth of CsPbBr₃ perovskite single-crystals in HBr has not been reported previously. In this work, constant temperature and controlled temperature lowering techniques were used to grow highly faceted CsPbBr₃ single-crystals.

Multiple nuclei formation could only be avoided by a precise temperature control. Disturbances of equilibrium conditions such as non-uniform temperature distribution or fast temperature lowering rates resulted in multi-nucleation, i.e., more than one single-crystals. Also, high synthesis temperatures increased the turbidity resulting in defects as observed by light microscope. It has also been shown that seeded growth is possible without foreign nucleation.

The formation of phase-pure orthorhombic CsPbBr₃ single-crystals was ensured by using a Cs to Pb ratio of 1.45 in the precursor solutions. XRF and EDS showed Cs-excess that, if not originating from the initial CsBr precursor (which is presumed to be washed away with HBr), might be from a Cs-rich cesium lead bromide phase such as Cs₄PbBr₆. However, the presence of secondary cesium lead bromide phases (such as CsPb₂Br₅, Cs₄PbBr₆) were not detected in XRD or DSC, though, they could be present below the instruments' detection limits. The UV-Vis-NIR diffuse reflectance graph is compatible with a semiconductor direct band gap. The band gap of 2.6 eV, which is consistent with literature, shows that it is suitable for the absorption in the visible region.

High quality CsPbBr₃ single-crystals are needed to understand the potential properties of CsPbBr₃. In this context, the parametric study done in this work offers deeper insight in the chemistry of single-crystal growth. Future research should focus on the growth of plate-like, centimeter-sized, clear CsPbBr₃ single-crystals for high energy photon detector applications.

Acknowledgement

The research was funded by Bursa Technical University-Scientific Research Projects Fund under grant number 182N26 and 200Y015. The authors thank MERLAB Bursa Technical University for the EDS and XRD measurements.

Author contributions

Murat Özen: Data curation, Conceptualization, Writing-Reviewing. **Cansu Akyel:** Data curation, Writing-Original draft preparation, Investigation. **Songül Akbulut Özen:** Visualization, Editing

Conflicts of interest

The authors declare no conflicts of interest.

References

1. Stoumpos, C. C., Malliakas, C. D., Peters, J. A., Liu, Z., Sebastian, M., Im, J., ... Kanatzidis, M. G. (2013). Crystal Growth of the Perovskite Semiconductor CsPbBr₃: A New Material for High-Energy Radiation Detection. *Crystal Growth & Design*, 13(7), 2722–2727. <https://doi.org/10.1021/cg400645t>
2. Liang, J., Liu, J., & Jin, Z. (2017). All-Inorganic Halide Perovskites for Optoelectronics: Progress and Prospects. *Solar RRL*, 1(10), 1700086. <https://doi.org/10.1002/solr.201700086>
3. Tailor, N. K., & Satapathi, S. (2020). The impact of Cs₃Bi₂Cl₉ single crystal growth modality on its symmetry and morphology. *Journal of Materials Research and Technology*, 9(4), 7149–7157. <https://doi.org/10.1016/j.jmrt.2020.04.097>
4. Yu, J., Liu, G., Chen, C., Li, Y., Xu, M., Wang, T., ... Zhang, L. (2020). Perovskite CsPbBr₃ crystals: Growth and applications. *Journal of Materials Chemistry C*, 8(19), 6326–6341. <https://doi.org/10.1039/D0TC00922A>
5. Li, S., Zhang, C., Song, J.-J., Xie, X., Meng, J.-Q., & Xu, S. (2018). Metal Halide Perovskite Single Crystals: From Growth Process to Application. *Crystals*, 8(5), 220. <https://doi.org/10.3390/cryst8050220>
6. Dang, Y., Ju, D., Wang, L., & Tao, X. (2016). Recent progress in the synthesis of hybrid halide perovskite single crystals. *CrystEngComm*, 18(24), 4476–4484. <https://doi.org/10.1039/C6CE00655H>
7. Dirin, D. N., Cherniukh, I., Yakunin, S., Shynkarenko, Y., & Kovalenko, M. V. (2016). Solution-Grown CsPbBr₃ Perovskite Single Crystals for Photon Detection. *Chemistry of Materials*, 28(23), 8470–8474. <https://doi.org/10.1021/acs.chemmater.6b04298>
8. Rakita, Y., Kedem, N., Gupta, S., Sadhanala, A., Kalchenko, V., Böhm, M. L., ... Hodes, G. (2016). Low-Temperature Solution-Grown CsPbBr₃ Single Crystals and Their Characterization. *Crystal Growth & Design*, 16(10), 5717–5725. <https://doi.org/10.1021/acs.cgd.6b00764>
9. Su, J., Chen, D. P., & Lin, C. T. (2015). Growth of large CH₃NH₃PbX₃ (X=I, Br) single crystals in solution. *Journal of Crystal Growth*, 422, 75–79. <https://doi.org/10.1016/j.jcrysgro.2015.04.029>
10. Dang, Y., Liu, Y., Sun, Y., Yuan, D., Liu, X., Lu, W., ... Tao, X. (2015). Bulk crystal growth of hybrid perovskite material CH₃NH₃PbI₃. *CrystEngComm*, 17(3), 665–670. <https://doi.org/10.1039/C4CE02106A>
11. Lian, Z., Yan, Q., Lv, Q., Wang, Y., Liu, L., Zhang, L., ... Sun, J.-L. (2015). High-Performance Planar-Type Photodetector on (100) Facet of MAPbI₃ Single Crystal. *Scientific Reports*, 5(1), 16563. <https://doi.org/10.1038/srep16563>
12. Peng, J., Xia, C. Q., Xu, Y., Li, R., Cui, L., Clegg, J. K., ... Lin, Q. (2021). Crystallization of CsPbBr₃ single crystals in water for X-ray detection. *Nature Communications*, 12(1), 1531. <https://doi.org/10.1038/s41467-021-21805-0>
13. He, Y., Matei, L., Jung, H. J., McCall, K. M., Chen, M., Stoumpos, C. C., ... Kanatzidis, M. G. (2018). High spectral resolution of gamma-rays at room temperature by perovskite CsPbBr₃ single crystals. *Nature Communications*, 9(1), 1609. <https://doi.org/10.1038/s41467-018-04073-3>
14. Zhang, H., Wang, F., Lu, Y., Sun, Q., Xu, Y., Zhang, B.-B., ... Kanatzidis, M. G. (2020). High-sensitivity X-ray detectors based on solution-grown caesium lead bromide single crystals. *Journal of Materials Chemistry C*, 8(4), 1248–1256. <https://doi.org/10.1039/C9TC05490A>
15. Altomare, A., Corriero, N., Cuocci, C., Falcicchio, A., Moliterni, A., & Rizzi, R. (2015). QUALX2.0: A qualitative phase analysis software using the freely available database POW_COD. *Journal of Applied Crystallography*, 48(2), 598–603. <https://doi.org/10.1107/S1600576715002319>
16. Gražulis, S., Daškevič, A., Merkys, A., Chateigner, D., Lutterotti, L., Quirós, M., ... Le Bail, A. (2012). Crystallography Open Database (COD): An open-access collection of crystal structures and platform for world-wide collaboration. *Nucleic Acids Research*, 40(D1), D420–D427. <https://doi.org/10.1093/nar/gkr900>
17. Zhang, H., Liu, X., Dong, J., Yu, H., Zhou, C., Zhang, B., ... Jie, W. (2017). Centimeter-Sized Inorganic Lead Halide Perovskite CsPbBr₃ Crystals Grown by an Improved Solution Method. *Crystal Growth & Design*, 17(12), 6426–6431. <https://doi.org/10.1021/acs.cgd.7b010>



© Author(s) 2023. This work is distributed under <https://creativecommons.org/licenses/by-sa/4.0/>